Optics Communications ▮ (▮▮▮▮) ▮▮▮–▮▮▮

Contents lists available at SciVerse ScienceDirect

Optics Communications

journal homepage: www.elsevier.com/locate/optcom

Calculation of the microscopic parameters of a self-induced transparency modelocked quantum cascade laser

Muhammad Anisuzzaman Talukder [a,b,*], Curtis R. Menyuk [a]

[a] Department of Computer Science and Electrical Engineering, University of Maryland, Baltimore County, 1000 Hilltop Circle, Baltimore, MD 21250, USA
[b] Department of Electrical and Electronic Engineering, Bangladesh University of Engineering and Technology, Dhaka 1000, Bangladesh

ARTICLE INFO

Article history:
Received 11 August 2012
Received in revised form
27 December 2012
Accepted 31 December 2012

Keywords:
Quantum cascade lasers
Self-induced transparency
Modelocking

ABSTRACT

A model to calculate the microscopic parameters of self-induced transparency (SIT) modelocked quantum cascade lasers (QCLs) is presented and the parameters are then calculated for a particular structure. These parameters are then used to calculate the gain to absorption ratio that is required to determine the required ratio of gain periods to absorbing periods that must be grown in order to obtain stable modelocked pulses. The modelocked pulse parameters, along with the stability limits are then calculated as the ratio of gain to absorption varies. For the SIT modelocked QCL design that we examined, we found that three to five gain periods must be grown for each absorbing period in order to ensure stable operation.

1. Introduction

Self-induced transparency (SIT) modelocking is a promising approach to create sub-ps pulses from mid-infrared quantum cascade lasers (QCLs) [1,2]. These pulses have the potential to play an important role in many mid-infrared (3.5−20 μm) applications, such as remote sensing, nonlinear frequency conversion, time-resolved measurements, coherent control, and frequency combs [3]. Fundamentally, it is difficult to create ultra-short pulses in QCLs using standard passive modelocking technique due to their fast gain recovery times T_1 ($\sim$1 ps) compared to the cavity round-trip time ($\sim$50 ps) and their narrow linewidths compared to that in other semiconductor lasers [4,5]. By contrast, stable pulses on the order of 100 fs can be obtained, in principle, from QCLs if they are modelocked using the SIT effect [1,2]. To modelock QCLs using the SIT effect, absorbing periods are grown in addition to the gain periods and interleaved with the gain periods. The absorbing periods help in the generation of stable pulses by absorbing the continuous waves and shaping the pulses as they propagate. Theoretical studies show that SIT-modelocked lasers are stable over a broad range of parameters. However, SIT-modelocked lasers do not self-start and must be injection-locked or seeded. Alternatively, it is possible to actively modelock the laser by modulating the input current to one of the segments in a two-segment laser as has been done in Ref. [3] for conventional QCLs that only have gain periods [6]. Preliminary experimental work to demonstrate the feasibility of this approach has been carried out [7].

In an SIT modelocked QCL, the ratio of the gain to the quantum coherent absorption, R_{ga}, that the pulses experience is an important parameter since it determines whether the laser operates stably. If R_{ga} is below a critical value, the gain is insufficient so that the pulses will damp. On the contrary, if R_{ga} is above a critical value, the absorption is insufficient to suppress the growth of the continuous waves, which may lead the generation of multiple pulses. The relationship between R_{ga} and the ratio between the number of gain periods and absorbing periods m_{ga} that must be grown is not simple and depends on the details of the design of these periods. Normally, the gain per gain period will be smaller than the absorption per absorbing period. From a practical standpoint, it is essential to calculate m_{ga} in order to grow SIT modelocked QCLs that operate stably.

In this paper, we show in detail for the first time how to calculate m_{ga} for a realistic set of parameters. This calculation is difficult because it depends on the quantum coherence between the quantum levels in the gain and absorbing periods. Standard design codes that do not take into account quantum coherence are insufficient. A full density matrix calculation must be made [8–10]. We note that this approach is more accurate than the rate-equation approach [11] that is commonly used to design QCLs. It is less accurate than Monte Carlo approaches [12]. However, it has computational advantage that it is sufficiently rapid computationally to be applied to realistic QCL structures.

It is necessary to use a multi-scale approach to make the problem computationally tractable. We first apply the density

* Corresponding author at: Department of Electrical and Electronic Engineering, Bangladesh University of Engineering and Technology, Dhaka 1000, Bangladesh.
E-mail address: anisuzzaman@umbc.edu (M. Anisuzzaman Talukder).

0030-4018/$ - see front matter © 2013 Elsevier B.V. All rights reserved.
http://dx.doi.org/10.1016/j.optcom.2012.12.094

matrix approach to a limited number of gain and absorbing periods with a realistic structure [2] to determine the microscopic parameters that are needed to find the gain per gain period and the absorption per absorbing period. That allows us to relate m_{ga} to R_{ga}. We then solve the Maxwell–Bloch equations [2] to determine the values of R_{ga} for which SIT modelocking is stable. The Maxwell–Bloch equations in effect average over the entire structure. Given R_{ga}, we can infer m_{ga} from the previous calculation. Multi-scale approaches like ours play an important role in modeling many solid-state devices [13,14].

In this work, we solve the Maxwell–Bloch equations applied to a two-level system. The Maxwell–Bloch equations applied to a two-level QCL model have proved sufficient in modeling experimentally observed phenomena [3–5], which is in contrast to the approach of Ref. [7] that solves the Maxwell–Bloch equations applied to a three-level system. We have solved the Maxwell–Bloch equations applied to a three-level system to determine the stability limits of SIT-modelocked QCLs. We found that the results using the three-level system are not significantly different than those obtained using a two-level system.

2. Theoretical modeling

The total gain per unit length (g) from the gain periods and the total absorption per unit length (a) from the absorbing periods of a QCL that has interleaved gain and absorbing periods are given by [1,2]

$$g=\frac{kN_g\Gamma_g\mu_g^2T_{2g}}{2\epsilon_0n^2\hbar},\quad a=\frac{kN_a\Gamma_a\mu_a^2T_{2a}}{2\epsilon_0n^2\hbar}. \tag{1}$$

In Eq. (1), subscripts g and a refer to a quantity in the gain and absorbing periods, respectively. The parameters N_g and N_a denote the total electron densities of the resonant levels of all the gain and absorbing periods. The parameters Γ_g and Γ_a denote the optical mode overlap in one gain period and one absorbing period. The parameters μ_g and μ_a denote the dipole moments between the resonant levels in the gain and absorbing periods. The parameters T_{2g} and T_{2a} denote the coherence times between the resonant levels in the gain and absorbing periods. The parameters k, ϵ_0, n, and $\hbar$ denote the wavenumber, the vacuum dielectric permittivity, the index of refraction, and the Planck's constant, respectively. Using Eq. (1), the ratio of gain to absorption per unit length of a QCL that has interleaved gain and absorbing periods is given by

$$R_{ga}=\frac{g}{a}=\frac{N_g\Gamma_g\mu_g^2T_{2g}}{N_a\Gamma_a\mu_a^2T_{2a}}. \tag{2}$$

The parameter R_{ga} can also be written as

$$R_{ga}=m_{ga}R'_{ga}, \tag{3}$$

where R'_{ga} is the ratio of the gain from one gain period g' to the absorption from one absorbing period a'. To calculate R'_{ga}, we replace N_g and N_a in Eq. (2) by N'_g and N'_a, respectively, where N'_g and N'_a are the carrier densities of the resonant levels in one gain period and one absorbing period, respectively. We assume that the optical mode overlaps equally in one gain period and one absorbing period, i.e., $\Gamma_g\approx\Gamma_a$. Therefore, we may write R'_{ga} as

$$R'_{ga}=\frac{g'}{a'}=\frac{N'_g\mu_g^2T_{2g}}{N'_a\mu_a^2T_{2a}}. \tag{4}$$

To calculate R'_{ga}, we have to calculate the carrier densities in the resonant levels, the dipole moments and the coherence times between the resonant levels in the gain and absorbing periods. A complete carrier transport calculation that includes all the energy levels in a period is required to calculate N'_g and N'_a. The carrier transport and hence the carrier distribution in the quantized energy levels is complicated since several different incoherent scattering and coherent tunneling processes are involved [15–18]. However, an accurate model of carrier transport in QCLs is needed for a number of applications besides SIT modelocking and is itself an active field of research [8,12,19,20]. To calculate the carrier densities, we use an extended density matrix formalism that includes carrier transport due to both incoherent scattering and coherent tunneling and is similar to the model that is discussed in [8–10]. However, we do not solve the carrier densities completely in k-space; instead, we average the scattering rates with a Fermi–Dirac distribution. The density matrix formulation that takes quantum coherence into account has been successful in reproducing experimentally observed phenomena [8–10]. We write the density equations as

$$\frac{dn_x}{dt}=\sum_{x'\neq x}\frac{n_{x'}}{s_{x'x}}-\sum_{x'\neq x}\frac{n_x}{s_{xx'}}-i\sum_{x'\neq x}\frac{\Delta_{0,xx'}}{2\hbar}(C_{xx'}-C^*_{xx'}), \tag{5a}$$

$$\frac{dC_{xx'}}{dt}=i\frac{\Delta_{0,xx'}}{2\hbar}(n_{x'}-n_x)-\frac{C_{xx'}}{T_{2,xx'}}-i\frac{E_{xx'}}{\hbar}C_{xx'}. \tag{5b}$$

In Eq. (5), the quantity n is the carrier density. Subscript x denotes an energy level. The quantity $C_{xx'}$ denotes the coherence between the energy levels x and x'. The coherence $C_{xx'}$ has a nonzero value only between an injector level and an active region level. The quantities $s_{xx'}$ and $T_{2,xx'}$ denote the scattering and coherence times between the energy levels x and x'. The parameter $\Delta_{0,xx'}$ denotes the energy splitting at resonance between the energy levels x and x' involved in coherent tunneling, while $E_{xx'}$ is the detuning of their energies from resonance.

We calculate $s_{xx'}$ from the intersubband electron–LO phonon (e–ph) and electron–electron (e–e) interactions, so that $1/s_{xx'}=1/s^{\mathrm{e-ph}}_{xx'}+1/s^{\mathrm{e-e}}_{xx'}$. Electron–LO phonon scattering dominates in intersubband transitions [21,22], but electron–electron scattering becomes important when the energy spacing between the levels is smaller than the LO phonon resonance energy, so that the LO phonon scattering is forbidden except for the electrons in the high energy tail [11]. We calculate μ_g and μ_a using an approach similar to that discussed in [23]. We calculate $T_{2,xx'}$ from intrasubband e–ph, e–e, and electron–interface roughness (e–ir) interactions, so that $1/T_{2,xx'}=1/T^{\mathrm{e-ph}}_{2,xx'}+1/T^{\mathrm{e-e}}_{2,xx'}+1/T^{\mathrm{e-ir}}_{2,xx'}$, where $T^{\mathrm{e-ph}}_{2,xx'}$, $T^{\mathrm{e-e}}_{2,xx'}$, and $T^{\mathrm{e-ir}}_{2,xx'}$ are the contributions to the coherence time $T_{2,xx'}$ due to e–ph, e–e, and e–ir interactions, respectively. The parameters $T^{\mathrm{e-ph}}_{2,xx'}$, $T^{\mathrm{e-e}}_{2,xx'}$, and $T^{\mathrm{e-ir}}_{2,xx'}$ are given by

$$\frac{1}{T^{\mathrm{e-ph}}_{2,xx'}}=\frac{1}{s^{\mathrm{e-ph,abs}}_{x\to x}}+\frac{1}{s^{\mathrm{e-ph,em}}_{x\to x}}+\frac{1}{s^{\mathrm{e-ph,abs}}_{x'\to x'}}+\frac{1}{s^{\mathrm{e-ph,em}}_{x'\to x'}}, \tag{6a}$$

$$\frac{1}{T^{\mathrm{e-e}}_{2,xx'}}=\frac{1}{s^{\mathrm{e-e}}_{x,x\to x,x}}+\frac{1}{s^{\mathrm{e-e}}_{x'x'\to x'x'}}, \tag{6b}$$

$$\frac{1}{T^{\mathrm{e-ir}}_{2,xx'}}=\frac{1}{s^{\mathrm{e-ir}}_{x\to x}}+\frac{1}{s^{\mathrm{e-ir}}_{x'\to x'}}-2\frac{1}{\sqrt{s^{\mathrm{e-ir}}_{x\to x}s^{\mathrm{e-ir}}_{x'\to x'}}}, \tag{6c}$$

where superscripts "abs" and "em" denote absorption and emission, respectively.

The implementation of the model starts with calculating the quantized energy levels and the associated wavefunctions of QCLs. To calculate the energy levels and the associated wavefunctions, we use the effective mass approach in the envelope function approximation and take nonparabolicity into account [23]. The calculated energy values and the associated wavefunctions are used to calculate the scattering and coherence lifetimes.

Please cite this article as: M. Anisuzzaman Talukder, C.R. Menyuk, Optics Communications (2013), http://dx.doi.org/10.1016/j.optcom.2012.12.094

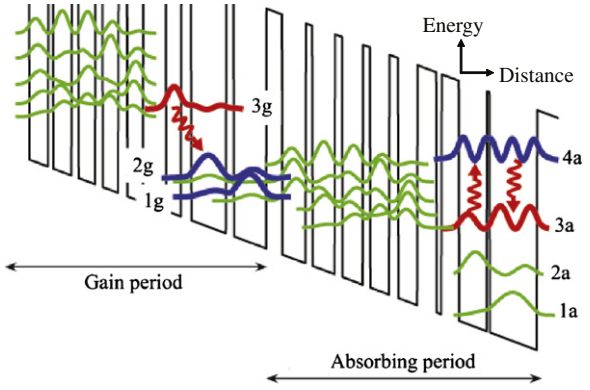

Fig. 1. Conduction band edge profile and the associated moduli-squared wavefunctions for interleaved one gain and one absorbing period of an SIT modelocked QCL. The sequence of layer dimensions is (in Å, starting from left): **42**, 34, **9**, 33, **12**, 30, **13**, 28, **16**, 28, **41**, 27, **18**, 62, **14**, 58, **28**, 42, **12**, 40, **13**, 37, **13**, 34, **16**, 34, **34**, 9, **31**, 50, **5**, 84. The numbers in bold type indicate $In_{0.52}Al_{0.48}As$ barrier layers and in roman type indicate $In_{0.53}Ga_{0.47}As$ well layers. Red wavy arrows indicate radiative transitions. The states that are numbered are in the active regions of the gain and absorbing periods. To differentiate the states in the gain and absorbing active regions, we append letters "*g*" and "*a*," respectively, with numbers. (For interpretation of the references to color in this figure caption, the reader is referred to the web version of this article.)

The electron–LO phonon and the electron–electron scattering rates are calculated using an approach that is discussed in [24], and the electron–interface roughness scattering rate is calculated using an approach that is discussed in [25]. To solve Eq. (5), we initially distribute the total carrier density in a period equally among the injector energy levels, and we leave the active region levels empty. We then solve Eq. (5) to obtain the steady-state values of the carrier densities. During the evolution of the carrier densities, the parameters $s_{xx'}$ and $T_{2,xx'}$ are recalculated as the carrier densities change.

3. Results

In Fig. 1, we show the conduction band edge diagram and the associated moduli-squared wavefunctions of the same SIT modelocked QCL design that was earlier presented and discussed in [1,2]. Here, we show one gain period and one absorbing period. In an actual structure there will be many such gain and absorbing periods. An appropriate choice of the numbers of gain and absorbing periods is necessary to obtain stable modelocked pulses. In the gain periods, levels 2*g* and 3*g* are the resonant levels, while in the absorbing periods, levels 3*a* and 4*a* are the resonant levels. To calculate g', the gain in a single period, we must calculate the carrier densities of levels 2*g* and 3*g*, and we must also calculate the dipole moment and the coherence time between levels 2*g* and 3*g*, from which we obtain $N'_g = n_{2g} + n_{3g}$, $T_{2g} = T_{2,2g\text{-}3g}$, and $\mu_g = \mu_{2g\text{-}3g}$. To calculate a', the absorption in a single absorbing period, we must calculate the carrier densities of levels 3*a* and 4*a*, and we must also calculate the dipole moment and the coherence time between levels 3*a* and 4*a*, from which we obtain $N'_a = n_{3a} + n_{4a}$, $T_{2a} = T_{2,3a\text{-}4a}$, and $\mu_a = \mu_{3a\text{-}4a}$. From g' and a', we then obtain $R'_{ga} = g'/a'$.

In this work, we assume that the total carrier density per gain period is equal to the total carrier density per absorbing period, which is 2×10^{11} cm^{-2}. We also assume an interface roughness height of 0.162 nm and an interface roughness correlation length of 6 nm in both the gain and absorbing periods. In the results presented here, we assume a temperature of 100 K. After solving Eq. (5), we find that $n_{2g} = 0.62 \times 10^{10}$ cm^{-2} and $n_{3g} = 5.84 \times 10^{10}$ cm^{-2}, so that, $N'_g = n_{2g} + n_{3g} = 6.50 \times 10^{10}$ cm^{-2}. We use the equilibrium values of n_{2g} and n_{3g} to calculate T_{2g}. We find that $T_{2g} \approx 15.7$ fs. In the absorbing periods, the upper resonant level 4*a* is far above the injector levels that are injecting current in the active region, so that we find that $n_{4a} \approx 0$. We find that $n_{3a} = 3.21 \times 10^{10}$ cm^{-2}. Therefore, $N'_a = n_{3a} + n_{4a} \approx n_{3a} = 3.21 \times 10^{10}$ cm^{-2}. We use the equilibrium values of n_{3a} and n_{4a} to calculate T_{2a}. We find that $T_{2a} \approx 45.5$ fs. From the equilibrium carrier densities of the resonant levels, we also find that the equilibrium population inversions in the gain and absorbing periods are 0.9 and -1, respectively. All these values correspond to realistic QCL structures [5–10].

We calculate the stability limits of the SIT modelocked QCL presented in Fig. 1 by solving the Maxwell–Bloch equations using an approach discussed in [2]. In the Maxwell–Bloch equations, we use the values of the coherence times and the population inversions in the gain and absorbing periods that we just calculated. To calculate the stability limits, we assume that the gain recovery times in the gain and absorbing periods are equal to 1 ps. We note that the gain recovery times in the gain and absorbing period will be on the order of ~ 1 ps, since we find that the carrier densities in the resonant levels reach steady-state in ~ 1 ps. The stability limits are given in Fig. 2 in terms of the normalized gain ($\bar{g}$) and the normalized absorption ($\bar{a}$) coefficients. Here, the gain and absorption coefficients are normalized by the linear loss (l), i.e., $\bar{g} = g/l$ and $\bar{a} = a/l$. We obtain stable modelocked pulses if the pair ($\bar{g}$, $\bar{a}$) corresponds to a point between the two solid (red) curves in Fig. 2. If the QCL operates with ($\bar{g}$, $\bar{a}$) above the upper curve, then the pulses damp. If the laser operates with ($\bar{g}$, $\bar{a}$) below the lower curve, then continuous waves grow.

We next substitute the values of N'_g, N'_a, μ_g, μ_a, T_{2g}, and T_{2a} into Eq. (4). We find $R'_{ga} \approx 0.2$. The operating point of the QCL will depend on the value of R_{ga}, which may be varied by changing the number of gain periods for each absorbing period. To obtain a value of $R_{ga} = 1$, five gain periods have to be grown for each absorbing period. In Fig. 2, we plot different lines within the stable operating limits that correspond to different choices of m_{ga}. If this QCL is grown with less than three gain periods per absorbing period, the pulses will damp. On the other hand, if this QCL is grown with more than five gain periods per absorbing period, continuous waves will grow.

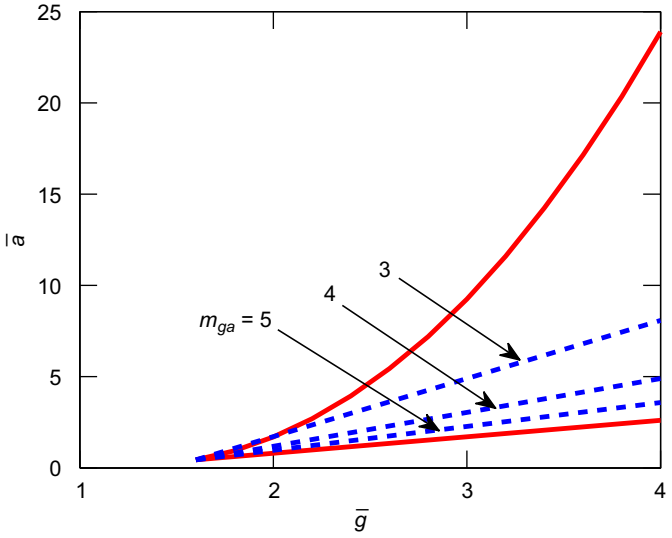

Fig. 2. Stability limits of normalized gain ($\bar{g}$) vs. normalized absorption ($\bar{a}$) for the SIT modelocked QCL design of Fig. 1. The laser is stable when operates between the two solid (red) curves. The dashed (blue) lines show the operating lines with different m_{ga}. (For interpretation of the references to color in this figure caption, the reader is referred to the web version of this article.)

Please cite this article as: M. Anisuzzaman Talukder, C.R. Menyuk, Optics Communications (2013), http://dx.doi.org/10.1016/j.optcom.2012.12.094

4. Conclusions

In conclusion, we have presented a multi-scale approach that allows us to calculate the ratio of the gain per gain period to the absorption per absorbing period in SIT modelocked QCLs. The model calculates the microscopic parameters using the density matrix formalism that takes quantum coherence into account; then the key macroscopic parameter, i.e., the ratio of gain to absorption, is calculated using the Maxwell–Bloch equations. We used the model to find R_{ga} as a function of m_{ga} for an SIT modelocked QCL design that has interleaved gain and absorbing periods. We have shown lines of constant m_{ga} as $\overline{g}$ and $\overline{a}$ are allowed to vary. We find that for this particular design, stable modelocked pulses can be obtained if three to five gain periods are grown for each absorbing period.

Acknowledgments

The authors gratefully acknowledge support from the MIRTHE Engineering Research Foundation, which is sponsored by the National Science Foundation. We thank Profs. F.-S. Choa, C. Gmachl, A. Johnson, and J. Khurgin for useful comments.

References

[1] C.R. Menyuk, M.A. Talukder, Physical Review Letters 102 (2009) 023903.
[2] M.A. Talukder, C.R. Menyuk, Physical Review A 79 (2009) 063841.
[3] C.Y. Wang, L. Kuznetsova, V.M. Gkortsas, L. Diehl, F.X. Kärtner, M.A. Belkin, A. Belyanin, X. Li, D. Ham, H. Schneider, P. Grant, C.Y. Song, S. Haffouz, Z.R. Wasilewski, H.C. Liu, F. Capasso, Optics Express 17 (2009) 12929.
[4] C.Y. Wang, L. Diehl, A. Gordon, C. Jirauschek, F.X. Kärtner, A. Belyanin, D. Bour, S. Corzine, G. Höfler, M. Troccoli, J. Faist, F. Capasso, Physical Review A 75 (2007) 031802.
[5] A. Gordon, C.Y. Wang, L. Diehl, F.X. Kärtner, A. Belyanin, D. Bour, S. Corzine, G. Höfler, H.C. Liu, H. Schneider, T. Maier, M. Troccoli, J. Faist, F. Capasso, Physical Review A 77 (2008) 053804.
[6] S.S. Shimu, A. Docherty, M.A. Talukder, C.R. Menyuk, Theoretical demonstration of stabilization of active modelocking in quantum cascade lasers with quantum coherent absorption, in: Proceedings of the 2012 IEEE Photonics Conference (IPC 2012), pp. 400.
[7] H. Choi, V.-M. Gkortsas, L. Diehl, D. Bour, S. Corzine, J. Zhu, G. Höfler, F. Capasso, F.X. Kärtner, T.B. Norris, Nature Photonics 4 (2010) 76.
[8] R. Terazzi, J. Faist, New Journal of Physics 12 (2010) 033045.
[9] M.A. Talukder, C.R. Menyuk, New Journal of Physics 13 (2011) 083027.
[10] M.A. Talukder, Journal of Applied Physics 109 (2011) 033104.
[11] D. Indjin, P. Harrison, R.W. Kelsall, Z. Ikonić, Journal of Applied Physics 91 (2002) 9019.
[12] C. Jirauschek, Applied Physics Letters 96 (2010) 011103.
[13] D.D. Vvedensky, Journal of Physics: Condensed Matter 16 (2004) R1537.
[14] P. Derosa, T. Cagin, Multiscale Modelling of Nanostructures, Taylor & Francis, New York, 2010.
[15] C. Sirtori, F. Capasso, J. Faist, A. Hutchinson, D. Sivco, A. Cho, IEEE Journal of Quantum Electronics 34 (1998) 1722.
[16] F. Eickemeyer, K. Reimann, M. Woerner, T. Elsaesser, Physical Review Letters 89 (2002) 047402.
[17] H. Choi, L. Diehl, Z.-K. Wu, M. Giovannini, J. Faist, F. Capasso, T.B. Norris, Physical Review Letters 100 (2008) 167401.
[18] A. Wacker, Physica Status Solidi (C) 5 (2008) 215.
[19] A. Gordon, D. Majer, Physical Review B 80 (2009) 195317.
[20] T. Kubis, C. Yeh, P. Vogl, Physica Status Solidi (C) 5 (2008) 232.
[21] R. Ferreira, G. Bastard, Physical Review B 40 (1989) 1074.
[22] M. Hartig, S. Haacke, B. Deveaud, L. Rota, Physical Review B 54 (1996) 14269.
[23] J. Faist, F. Capasso, C. Sirtori, D.L. Sivco, in: H.C. Liu, F. Capasso (Eds.), Intersubband Transitions in Quantum Wells: Physics and Device Applications II, Academic Press, San Diego, CA, 2000, p. 1.
[24] J.H. Smet, C.G. Fonstad, Q. Hu, Journal of Applied Physics 79 (1996) 9305.
[25] T. Unuma, M. Yoshita, T. Noda, H. Sakaki, H. Akiyama, Journal of Applied Physics 93 (2003) 1586.

Please cite this article as: M. Anisuzzaman Talukder, C.R. Menyuk, Optics Communications (2013), http://dx.doi.org/10.1016/j.optcom.2012.12.094